presumed to be the inverse of a Hermitian (real eigenvalues) operator. Nonautoionizing states with $E_j>0$ have poles on the branch cut and could modify the conclusions which have been drawn, since for such states the sign of $E-E_j$ appearing in Eq. (21) need not be positive. It can be proved however that for such states the integrals appearing in Eq. (20) necessarily vanish [note $\alpha_j$ is now imaginary, equals $ik_j$, where $k_j$ is defined in terms of $E_j$ by Eq. (14)]. Consequently such nonautoionizing states cannot contribute to the dispersion relations.

## V. CONCLUSIONS

In the light of the foregoing discussion the following assertions seem justified. If experiment F is taken to be correct the angular distribution should change smoothly with energy, and must be considerably peaked at low energies. If experiment B is correct, the angular distribution must change rapidly from a very broad or even sideways peaked shape to a highly forward peaked distribution, in a narrow range of energies near 13.6 ev. Dispersion relations are not able to rule out either experiment B or F, but do suggest the experiment which will distinguish between them, namely: angular distribution measurements at low energies. A closer distinction would be possible if there were more accurate measurements of the total cross sections at high energies, which would obviate the need for extrapolations and increase the reliability of the computed dispersion integral. Direct information on combinations of $f$ and $g$ other than $f-\frac{1}{2}g$, e.g., direct measurement of $|g|^2$ by polarized atomic beam techniques,[17] also would be helpful.

## ACKNOWLEDGMENTS

We are indebted to E. Sobolak and Dr. R. Drisko for pointing out an important error in a preprint of this paper. Correction of this error greatly modifies assertions made previously.[18]

[17] K. Rubin, J. Perel, and B. Bederson, Phys. Rev. **117**, 151 (1960).
[18] N. A. Krall and E. Gerjuoy, Bull. Am. Phys. Soc. Ser. II, **5**, 119 (1960).

PHYSICAL REVIEW VOLUME 119, NUMBER 2 JULY 15, 1960

# Cross Section for Formation of Doubly-Ionized Helium by Electron Impact*

H. E. STANTON AND J. E. MONAHAN
*Argonne National Laboratory, Lemont, Illinois*
(Received March 7, 1960)

The cross section for the formation of $He^{++}$ by electron impact has been measured relative to that of $He^{+}$ for electron energies between 100 ev and 2400 ev. A relative minimum in the measured ratio of the yields of $He^{+}$ to $He^{++}$ at an energy of about 600 ev is believed to be real. For incident energies above 1400 ev the results are consistent with a constant value of 145 for this ratio.

## INTRODUCTION

THE cross section for ionization of helium by electron impact has been measured by Smith[1] for electron energies between the appearance potential and about 4000 ev. Since the quantity actually measured by Smith is the ratio of positive-ion current produced in the helium gas to the current of the penetrating electrons, it is necessary to know the fraction of the positive current associated with each type of ion, $He^{+}$ and $He^{++}$, in order to deduce the cross sections $Q_i$ and $Q_{ii}$ for single and double ionization, respectively. Apparently the only measurement of this ratio is that reported in 1936 by Bleakney and Smith.[2] These latter authors measured the relative yield of doubly-charged helium ions for a range of incident electron energies from 100 ev to 500 ev. In order to relate these measurements to an absolute cross section, they measured the ratio of the yields of $He^{+}$ to $He^{++}$ at an energy of 300 ev.

The only theoretical calculation pertaining to the process of double ionization in helium seems to be Ninti's[3] estimate of an upper limit for the sum of oscillator strengths for simultaneous excitation or ionization involving both electrons. As pointed out by Miller,[4] a value of the oscillator strength for double excitation of the order of magnitude of Ninti's estimate would indicate that double excitations play a considerable role in many processes, particularly those that depend sensitively on the energy transfer between initial and final states.

In this paper are described the results of measurements of the ratio of yields of $He^{+}$ and $He^{++}$ for electron energies between 100 ev and 2400 ev. One problem considered for these measurements at higher energies

* Work performed under the auspices of the U. S. Atomic Energy Commission.
[1] P. T. Smith, Phys. Rev. **36**, 1292 (1930). Experimental points determined by W. Hanle and D. Riede, Z. Physik **133**, 537 (1952) are included in Fig. 1.
[2] W. Bleakney and L. Smith, Phys. Rev. **49**, 402 (1936).
[3] J. P. Ninti, Phys. Rev. **42**, 632 (1932).
[4] William F. Miller, Ph.D. thesis, Purdue University, January, 1956 (unpublished).

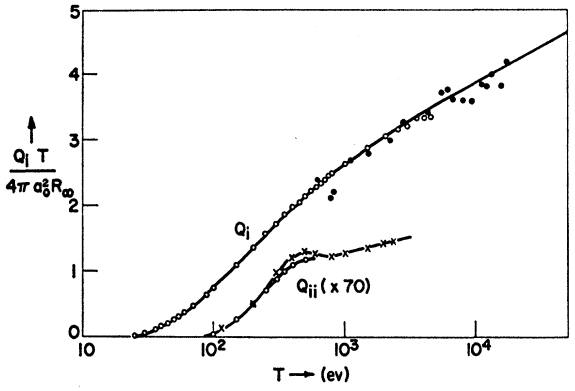


FIG. 1. The cross section for formation of the singly-charged helium ion ($Q_i$) or the doubly-charged ion ($Q_{ii}$) multiplied by the kinetic energy ($T$) of the bombarding electron. Abscissa is the kinetic energy ($T$) of the bombarding electrons. Points marked × for $Q_{ii}$ were calculated from the present work by using the curve for $Q_i$ as known. The other points are experimental values published in the references.

is the determination of the squared modulus of the matrix element of the dipole moment for the transition from the ground state to states of the doubly-ionized continuum. The results seem to indicate that Ninti's estimate of the oscillator strength for double ionization is of the correct order of magnitude.

The results of the investigations of Smith[1] and Bleakney and Smith[2] have been synthesized by Miller and are shown in Fig. 1, together with some of the results of the present investigation. The cross section for double ionization was obtained by dividing Smith's results by the measured ratio of the yield of $He^+$ to that of $He^{++}$.

## EXPERIMENTAL

The energy-selecting mass spectrometer,[5] shown in Fig. 2, was used to measure the yields of the two ionic species of helium. The energy-selecting feature was effectively eliminated by sweeping over the entire peak and thus integrating the ion intensity for all energies. The arrangement of the electron source and focusing-slit plates is shown in Fig. 3. For the higher bombarding energies, the focusing was sufficiently sharp that more than 95% of the electrons passed through the ion box and were caught in the trap. The resulting trap current was maintained at a constant value for any given measurement of the yield ratio. Electron currents from 0.1 to 20 $\mu$a were used; however, for most of the work, an electron current of 2.0 $\mu$a was used.

As shown in Fig. 2 the ion beam was extracted from the ion box at right angles to the incident electron beam, focused through the energy analyzer, and then analyzed for mass. The total ion current was monitored after issuing from the energy analyzer, as was the final current after passage through the mass analyzer. The detection of the final ion current employed pulse-counting techniques. The individual ions entering the multiplier produced greatly amplified pulses from the output of the multiplier. These pulses were subsequently amplified and the counting rate determined by conventional means. By this method, mass and energy discriminations arising from variation in the numbers of secondary electrons produced on the dynodes were eliminated.

Since the focus of the electrons through the ion box determines the shape of the incident beam, the procedure was to disturb these focusing adjustments as little as possible in changing the mass-to-charge ratio from $m/e=2^+$ to $m/e=4^+$. The change in the selected mass-to-charge ratio was accomplished by adjusting the magnetic field and this necessitated a slight readjustment of the focusing in order to compensate for the perturbations due to the stray magnetic field.

The energy of the incident electron beam was varied from 100 ev to 2400 ev in steps of roughly 100 ev. Each measurement of the ion yield consisted of a sweep across the peak of ion energy for both increasing

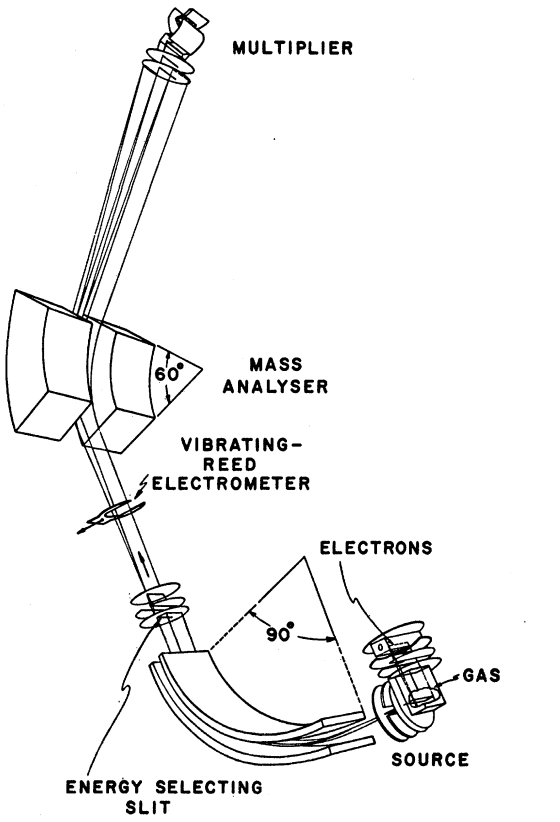


FIG. 2. Mass spectrometer used in the experimental measurements shown in perspective. Ions formed in the gas chamber pass through a pair of cylindrical electrodes, where energy analysis takes place, and then through the magnetic field where mass separation takes place. Detection is at the top of the figure and was accomplished by a multiplier. The total length of path traveled by the ions was approximately 6 ft.

[5] The details of this spectrometer are described in H. E. Stanton, J. Appl. Phys. (to be published).

and decreasing energy and, in addition, an evaluation of the relevant backgrounds. Since the total number of ions registered in an energy sweep did not repeat very well from day to day, attempts to evaluate the cross sections directly from the integrated yields, the electron current, and the source pressure were not successful. The ratio of the yields of $He^+$ and $He^{++}$ was considerably more stable over long periods of time and, since the cross section for the yield of $He^+$ is known over this energy interval, attention was concentrated on the measurement of this ratio.

Throughout the investigation the ion intensity for the peak at $m/e=2^+$ was uncomfortably low. This counting rate had to be maintained at a low level in order to prevent saturation of the counting equipment by the $He^+$ ion. Attempts were made to compensate for this by increasing the electron current for the measurements involving the $He^{++}$ ion and, at the same time, increasing the pressure of the helium gas in the source. However, because of nonlinearities in the spectrometer this procedure did not give as reliable data as were obtained when the source conditions were maintained as nearly constant as possible for the two ionic species.

The results are shown in Fig. 4. Some of the earlier runs had $N_2$ added to the helium gas in order to increase the intermediate beam current. This practice was abandoned because it was feared that the helium ions would recover electrons from the nitrogen molecule and thus introduce a systematic error in the measured yield ratio. Within the inherent scatter of the experimental points this seems not to be the case and these data were included in Fig. 4.

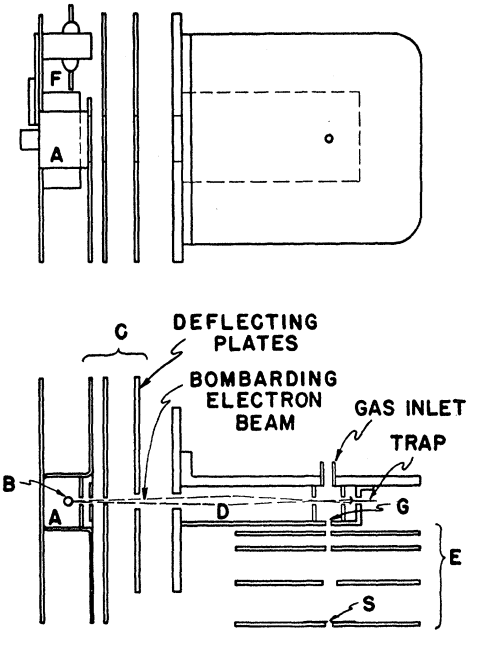


FIG. 3. The ion source used. This comprised an assembly of slits, $C$, to accurately focus the electron beam on the trap after passing through the gas chamber. The helium ions were withdrawn at right angles through the slit $G$, and focused on the source slit $S$ (0.004 in.$\times\frac{9}{16}$ in.) by the slit system $E$. The electrons were supplied by a filament $B$ parallel to the slits in the assembly $C$.

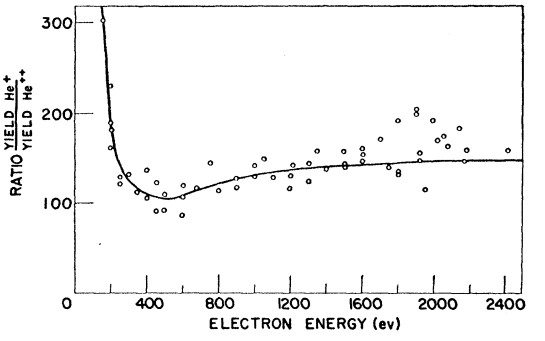


FIG. 4. The experimental values of the ratio of yields of the two ionic species of helium under electron impact as a function of the electron energy. The points were obtained by changing electron energies in increments of from 100 ev to 200 ev, between successive single determinations throughout the range of study, not by determining the ratio several times at a given setting of the electron energy.

## DISCUSSION OF RESULTS

The magnitude of the scatter in the observed values of the ratio of the $He^+$ yield to $He^{++}$ yield is considerably larger than would be expected from the usual counting statistics. Therefore, it is necessary to determine, as well as possible, the nature of the uncertainties inherent in the data. Any averaging procedure is justified only if a reasonable approximation to the distribution of these "errors" can be determined.

Since successive energy-selecting runs for a given mass-to-charge ratio consistently repeated to within less than 10%, it was assumed that the major source of error occurred in shifting from one mass to the other. This involved changing the mass-analyzing magnetic field, readjusting (trimming) the ion-accelerating voltage to maximize the ion intensity, and slightly readjusting the focusing of the electron beam. The most sensitive of these readjustments is the trimming of the ion-accelerating voltage. The ion intensity as a function of accelerating voltage is shown in Fig. 5. The peaks for both $He^+$ and $He^{++}$ are reasonably flat in the neighborhood of their maxima so that the high voltage could be set within certain tolerances and still give accurate results. Unfortunately, however, sweeping the voltage of the energy selector, in effect integrating over the energy spectrum of the ion of interest, is equivalent to sweeping over a region of the intensity peak in Fig. 5. Thus a slight misadjustment or shift in the high voltage would reduce the integrated ion current below its proper value.

The results plotted in Fig. 5 show that the ionic yield $Y$ as a function of $x$, the deviation of the accelerating voltage from its proper setting, is given to a

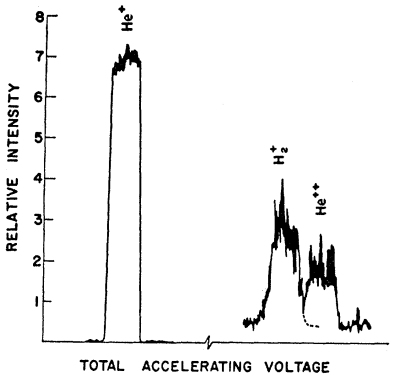


FIG. 5. The actual shapes of the peaks for $He^+$ and $He^{++}$ as recorded as a function of the main accelerating voltage. The right tracing for $H_2^+$ and $He^{++}$ was made with greatly increased detector sensitivity and cannot be compared directly in intensity with the peak for $He^+$. The $H_2^+$ peak arose from background gases. The width at half maximum of each peak is from 15 to 20 v. The average total accelerating potential used was 8 kv for both ions.

good approximation by an expression of the form

$$Y^{(j)}(x)=Y_M{}^{(j)}(1-x^2/a^2)+Y_m{}^{(j)}x^2/a^2, \quad |x|\leqslant a$$
$$=0, \quad |x|>a \qquad (1)$$

for both $He^+$ ($j=1$) and $He^{++}$ ($j=2$). Here $Y_M$ and $Y_m$ denote the maximum and minimum values of the ionic yield, respectively. In evaluating the ratio of these yields, the experimental procedure was equivalent to the random selection of a value of $x$ that determined the yield of one ionic species and an independent selection of a value of $x$, again at random, that determined the yield of the second ionic species. Thus the distribution function of $x$ is given as

$$f(x)dx=dx/2a, \quad |x|\leqslant a.$$
$$=0 \quad |x|>a. \qquad (2)$$

In the following it is convenient to discuss the ratio of the yield of $He^{++}$ to that of $He^+$, i.e., $R=Y^{(2)}/Y^{(1)}$ The quantity $Pr[R\leqslant r]$, the probability that an observed value of this ratio does not exceed a preassigned value $r$, is given by the distribution function

$$\mathfrak{F}(r)=\int\int_S dy\,dy'\,F^{(1)}(y)F^{(2)}(y'), \qquad (3)$$

where $S$ is the set of points, in the $yy'$ plane, satisfying the inequalities $Y_m{}^{(1)}\leqslant y\leqslant Y_M{}^{(1)}$, $Y_m{}^{(2)}\leqslant y'\leqslant Y_M{}^{(2)}$, and $y'\leqslant ry$ and

$$F^{(j)}(y)=\tfrac{1}{2}(Y_M{}^{(j)}-Y_m{}^{(j)})^{-\frac{1}{2}}(Y_M{}^{(j)}-y)^{-\frac{1}{2}}, \quad j=1, 2. \qquad (4)$$

When Eq. (1) is fitted to the intensity distributions shown in Fig. 5, the values of the constants to be used in evaluating Eq. (3) are found to be

$$Y_m{}^{(1)}/Y_M{}^{(1)}=0.9, \quad Y_m{}^{(2)}/Y_M{}^{(2)}=0.6. \qquad (5)$$

The only variable which remains unspecified in Eq. (3) is conveniently taken to be $Y_M{}^{(2)}/Y_M{}^{(1)}$, the "true" value of the ratio $R$.

A histogram of the distribution of the experimentally observed ratios for electron energies above 1400 ev is shown in Fig. 6. If it is assumed that the true value of $R$ is essentially constant for bombarding energies above 1400 ev, this histogram is just the experimentally observed distribution function $\mathfrak{F}(r)$. The smooth curve in Fig. 6 was obtained from Eq. (3) for a "true" value $Y_M{}^{(1)}/Y_M{}^{(2)}=0.0069$. The good agreement between the experimental distribution and the calculated one indicates that the spectrometer variations described by Eq. (3) could account for the scatter observed in the data. In these calculations the errors resulting from the refocusing of the electron beam were not taken into account explicitly. However, if these are of small importance in comparison with the uncertainties in the high-voltage adjustment, as we believe they are, then these added sources of error are adequately included by a small adjustment in the range of the distribution given by Eq. (3), i.e., by the choice of values given by Eq. (5).

If the distribution function shown in Fig. 6 is assumed to be an adequate approximation for the distribution of the major sources of error in these measurements and if the same distribution can be extrapolated to the entire range of bombarding energies, then the most probable values of the ratio $Y_M{}^{(2)}/Y_M{}^{(1)}$ are those on the smooth curve shown in Fig. 4. The relative minimum in this curve in the vicinity of 500 ev appears to be real and independent of any assumptions concerning error distributions. Most series of measurements were made by starting with low electron energies and proceeding to successively higher ones, or vice versa. All of the runs that covered a sufficiently large energy range reproduced this minimum. It is difficult to attribute this behavior to anything associated with the spectrometer. All of the various electrode voltages were left practically untouched throughout this investigation and the adjustment of the ion-accelerating voltage, although possibly producing a large scatter, would not be expected to give a consistently reproducible minimum at a given energy.

If the values $Y_M{}^{(2)}/Y_M{}^{(1)}$ shown in Fig. 4 are divided into the cross section for the yield of $He^+$ as determined from the measurements of Smith, the cross section $Q_{ii}$ for the yield of $He^{++}$ is obtained. The curve of $Q_{ii}$ as a function of bombarding energy has been included in Fig. 1 and agrees reasonably well with the double-ionization results reported by Bleakney and Smith over the energy interval common to both measurements. However, the cross section obtained from the present work seems to be about 10–15% higher than that observed by Bleakney and Smith. It should be mentioned that the relative standard deviation in the ratio $Y_M{}^{(2)}/Y_M{}^{(1)}$ predicted by the distribution defined by Eq. (3) is about 10%.

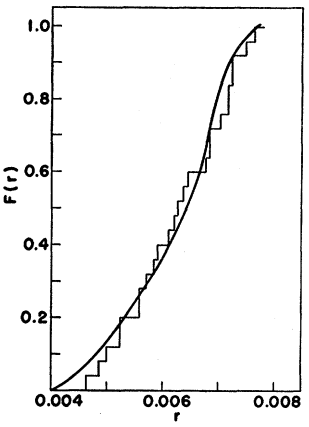


FIG. 6. The histogram derived from data shown in Fig. 4. The smooth curve is a plot of Eq. (3) with the values given in Eq. (5) which were obtained from the shape of the peaks, shown in Fig. 5.

The broad "resonance" in the cross section for the production of $He^{++}$ in the vicinity of 500 ev is, of course, a result of the extremum in the measured ratio at these energies. It is tempting to attribute this extremum to structure of the cross section for the yield of $He^{+}$; however, it is very difficult to justify this interpretation in the light of Smith's measurements. The remaining alternative is the possibility of a band of final doubly ionized states which produce a "resonance" effect in the interaction matrix.

The Born approximation to the cross section for the yield of $He^{+}$ is known[4] to reproduce the measured values quite accurately for electron energies above 1000 ev. Since the cross section for the production of $He^{++}$ shows every indication of having reached its asymptotic form at an energy of 1400 ev, we have attempted to fit the values of $R$ observed for energies above 1400 ev to the ratio predicted by the Born approximation,[6] namely,

$$Y_M^{(2)}/Y_M^{(1)}=(M_{ii}^2 \ln 4T+C_{ii})/Q_i(T), \qquad (6)$$

where $M_{ii}^2$ is the squared modulus of the matrix element of the dipole moment between the ground and doubly-ionized states of helium, $C_{ii}$ is a constant depending on properties of the final states of the system, and $Q_i(T)$ is the measured cross section for the yield of $He^{+}$ at a bombarding energy $T$. If we let

$$d\mathfrak{F}/dr=f(r|Y_M^{(2)}/Y_M^{(1)}),$$

where $\mathfrak{F}$ is defined by Eqs. (3) and (5) and the ratio $Y_M^{(2)}/Y_M^{(1)}$ is given by Eq. (6), the likelihood function for the observed values $r_\alpha$ of this ratio for $T>1400$ ev is defined as

$$\mathfrak{L}(M_{ii}^2,C_{ii})=\prod_\alpha f(r_\alpha|M_{ii}^2,C_{ii}), \qquad (7)$$

where the product is over all observations $\alpha$. Since the distribution function is specified by a formally different expression for different intervals in $r$, it is not a simple matter to carry out the formal manipulations which are required in order to obtain the maximum-likelihood estimates for $M_{ii}^2$ and $C_{ii}$. On the other hand, the same information may be obtained by evaluating Eq. (7) for a range of values of $M_{ii}^2$ and $C_{ii}$. In this manner we find that $\mathfrak{L}(M_{ii}^2,C_{ii})$ has a maximum for $M_{ii}^2=0.003$ and $C_{ii}=0.002$. However, this maximum is quite broad for values of $M_{ii}^2$ and $C_{ii}$ which satisfy the linear relation

$$M_{ii}^2=0.313\times10^{-2}-0.164C_{ii}, \qquad (8a)$$

where for the values

$$|C_{ii}+0.002|=0.006,$$

the function $\mathfrak{L}$ is reduced to 50% of its maximum value.

As mentioned previously, the only theoretical calculation pertaining to the process of double ionization in helium is Ninti's estimate of 0.007 as an upper limit for the matrix element $M_{ii}^2$. More specifically, Ninti's estimate is for the process of double excitation so that, taken literally, our upper limit of $M_{ii}^2=0.004$ would imply that a relatively large fraction of double excitations do not result in double ionization.

## ACKNOWLEDGMENTS

We wish to express our sincere appreciation to Dr. W. F. Miller for numerous very helpful discussions in the interpretation of the results and their theoretical implications during the latter stages of the investigation.

We also wish to thank Dr. Robert Platzman for his interest in the problem during the early stages of the experimental work.

[6] Atomic units are used throughout the remainder of this discussion, i.e., energies are given in units of the rydberg and distances in units of the radius of the first Bohr orbit in hydrogen.